

Syntheses, spectral, X-ray and DFT studies of 5-benzyl-N-phenyl-1,3,4-thiadiazol-2-amine, 2-(5-phenyl-1,3,4-thiadiazol-2-yl) pyridine and 2-(5-methyl-1,3,4-thiadiazole-2-ylthio)-5-methyl-1,3,4-thiadiazole obtained by Mn(II) catalyzed reactions



R.K. Dani^a, M.K. Bharty^{a,*}, S.K. Kushawaha^a, S. Paswan^a, Om Prakash^b, Ranjan K. Singh^b, N.K. Singh^a

^a Department of Chemistry, Banaras Hindu University, Varanasi 221005, India

^b Department of Physics, Banaras Hindu University, Varanasi 221005, India

HIGHLIGHTS

- Substituted thiosemicarbazide/thiohydrazide get cyclized into thiadiazole in the presence of manganese(II) salt.
- The compounds are stabilized through intramolecular and weak intermolecular hydrogen bonding.
- X-ray crystallographic results are well produced by DFT calculations.
- The HOMO and LUMO energies of the molecules are negative indicating that the all compounds are stable.
- Lower energy gap for the compound **2** indicates better NLO properties as compared to compounds **1** and **3**.

ARTICLE INFO

Article history:

Received 22 July 2013

Received in revised form 26 September 2013

Accepted 26 September 2013

Available online 4 October 2013

Keywords:

1,3,4-Thiadiazole derivatives
Mn(II) catalyzed conversion
NLO
DFT calculation

ABSTRACT

New compounds 5-benzyl-N-phenyl-1,3,4-thiadiazol-2-amine (Bptha, **1**), 2-(5-phenyl-1,3,4-thiadiazol-2-yl) pyridine (Pthp, **2**) and 2-(5-methyl-1,3,4-thiadiazole-2-ylthio)-5-methyl-1,3,4-thiadiazole (Mtmth, **3**) have been synthesized and characterized with the aid of elemental analyses, IR, NMR and single crystal X-ray data. The structure of compounds **1**, **2** and **3** are stabilized *via* intramolecular as well as intermolecular hydrogen bonding and crystallize in monoclinic system with space group P 1, P21/n and P 1, respectively. During the course of reaction, the substituted thiosemicarbazide/thiohydrazide get cyclized into the corresponding thiadiazole in the presence of manganese(II) nitrate *via* loss of H₂O to yield compounds **1** and **2**. However condensation occurred in the case of 5-methyl-1,3,4-thiadiazole-2-thiol which yielded 2-(5-methyl-1,3,4-thiadiazole-2-ylthio)-5-methyl-1,3,4-thiadiazole (**3**) by loss of one mole of H₂S from two moles of 5-methyl-1,3,4-thiadiazole-2-thiol in the presence of manganese(II) acetate. The geometry optimization has been performed using DFT method and geometrical parameters thus obtained for the compounds have been compared with their single crystal X-ray data. The negative values of HOMO and LUMO energies for the molecules indicate that they are stable. The electronic transition from the ground state to the excited state due to a transfer of electrons from the HOMO to LUMO levels is mainly associated with the $\pi \rightarrow \pi^*$ transition.

© 2013 Elsevier B.V. All rights reserved.

1. Introduction

1,3,4-Thiadiazole and its derivatives have found applications as bioactive agents such as antimicrobials, antituberculostatic, anti-inflammatory, analgesic, antifungal, antipyretic and anticonvulsant [1–9]. The synthesis of this type of heterocyclic compounds has attracted considerable attention and several methods have been developed for their syntheses, for example the oxidative

cyclization of acyclic precursor such as N'-acyl hydrazine-carbo-dithioic acid alkyl ester [10,11]. 1,3,4-Thiadiazoles are used as starting material for the synthesis of numerous types of chemical compounds including sulfa drugs, biocides, fungicides, dyes and chemical reaction accelerators [12]. Thiadiazoles containing mercapto, hydroxyl and amino substituents can exist in tautomeric forms and have found many industrial applications and possess surprising chemical properties including their capacity for forming complexes with metal ions [13]. These properties prompted us to synthesize a new type of heterocyclic compound with a presumption that incorporation of phenyl and pyridine rings in the thiadiazole moiety would have much better solubility in non-aqueous

* Corresponding author. Tel.: +91 542 6702447.

E-mail address: mkbharty@bhu.ac.in (M.K. Bharty).

medium. Here we report the metal assisted cyclization of 4-phenyl-1-(2-phenylacetyl) thiosemicarbazide and *N'*-benzothioylpicolinohydrazide to 5-benzyl-*N*-phenyl-1,3,4-thiadiazol-2-amine and 2-(5-phenyl-1,3,4-thiadiazol-2-yl) pyridine, respectively, during an attempt to prepare their complexes with manganese (II) nitrate. The conversion of 5-methyl-1,3,4-thiadiazole-2-thiol to 2-(5-methyl-1,3,4-thiadiazole-2-ylthio)-5-methyl-1,3,4-thiadiazole has been achieved under mild condition using manganese(II) acetate. The spectroscopic, single crystal X-ray structure, DFT studies, FMOs analysis and NLO properties of the resulting compounds are presented in this paper.

2. Experimental section

2.1. Materials and physical measurements

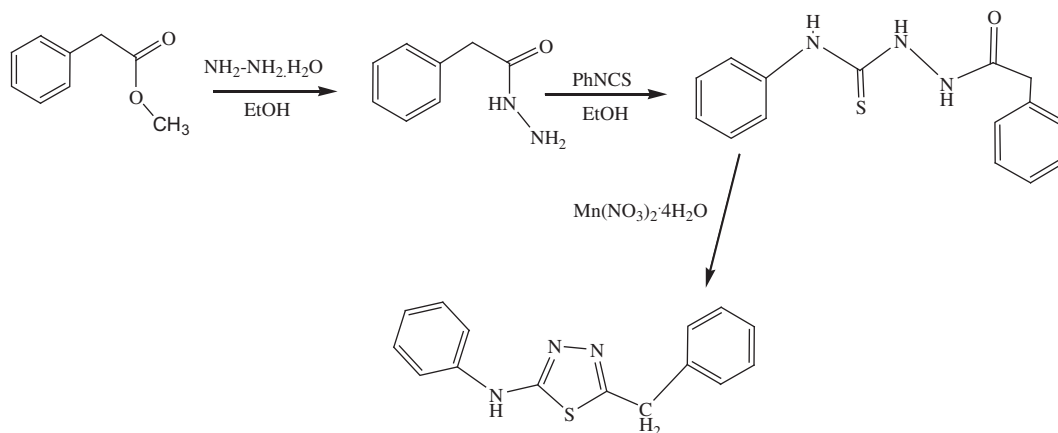
Commercial reagents were used without further purification and all experiments were carried out in open atmosphere. Methyl-2-phenyl acetate, picolinic acid hydrazide, hydrazine hydrate (SD Fine Chemicals, India), phenyl isothiocyanate and

5-methyl-1,3,4-thiadiazole-2-thiol (Sigma Aldrich) were used as received. The 2-phenyl acetohydrazide was prepared by refluxing equimolar amount of methyl-2-phenyl acetate with hydrazine hydrate. All the solvents were purchased from Merck Chemicals, India, and used after purification. Carbon, hydrogen, nitrogen and sulfur contents were estimated on a CHN Model CE-440 Analyser and on an Elementar Vario EL III Carlo Erbo 1108. IR spectra were recorded in the 4000–400 cm^{-1} region as KBr pellets on a Varian Excalibur 3100 FT-IR spectrophotometer. ^1H and ^{13}C NMR spectra were recorded in $\text{DMSO}-d_6$ on a JEOL AL300 FT NMR spectrometer using TMS as an internal reference.

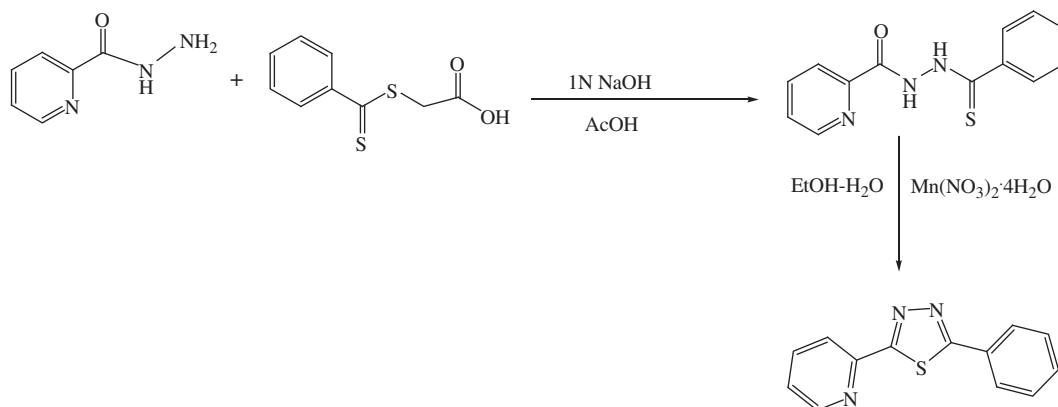
2.2. Synthesis

2.2.1. Synthesis of 5-benzyl-*N*-phenyl-1,3,4-thiadiazol-2-amine (Bptha, **1**)

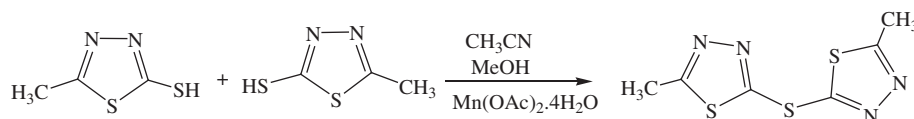
A mixture of 2-phenyl acetohydrazide (1.220 g, 10 mmol) and phenyl isothiocyanate (1.2 mL, 10 mmol) in absolute ethanol (20 mL) was refluxed for 6 h at 70 °C. The solid 4-phenyl-1-(2-phenylacetyl) thiosemicarbazide obtained upon cooling was



Scheme 1. Synthesis of 5-benzyl-*N*-phenyl-1,3,4-thiadiazol-2-amine (Bptha).



Scheme 2. Synthesis of 5-benzyl-*N*-phenyl-1,3,4-thiadiazol-2-amine (Pthp).



Scheme 3. Synthesis of 2-(5-methyl-1,3,4-thiadiazole-2-ylthio)-5-methyl-1,3,4-thiadiazole (Mtmth).

Table 1
Crystallographic data for the compound **1**, **2** and **3**.

Parameters	1	2	3
Empirical formula	C ₁₅ H ₁₃ N ₃ S	C ₁₃ H ₉ N ₃ S	C ₆ H ₆ N ₄ S ₃
Formula weight	267.35	239.30	230.36
Crystal system	Monoclinic	Monoclinic	Monoclinic
Space group	P1	P2 ₁ /n	P1
T (K)	293(2)	293(2)	293(2)
λ, Mo Kα (Å)	0.71073	0.71073	0.71073
a (Å)	11.3408(19)	14.1797(15)	5.6970(6)
b (Å)	7.0518(10)	16.5084(17)	6.7973(10)
c (Å)	8.5427(10)	15.970(2)	12.0017(13)
β (°)	103.887(14)	110.866(13)	102.569(10)
V (Å ³)	663.22(17)	3493.2(7)	453.62(10)
Z	2	12	2
ρ _{calcd} (g/cm ³)	1.339	1.365	1.686
μ (mm ⁻¹)	0.233	0.256	0.770
F(000)	280	1488	236
Crystal size (mm ³)	0.23 × 0.21 × 0.18	0.27 × 0.23 × 0.21	0.28 × 0.24 × 0.20
θ range for data collections (°)	3.41–29.23	3.31–29.05	3.00–29.16
Index ranges	–14 ≤ h ≤ 15 –9 ≤ k ≤ 9 –10 ≤ l ≤ 11	–25 ≤ h ≤ 24 –23 ≤ k ≤ 22 –19 ≤ l ≤ 18	–7 ≤ h ≤ 7 –8 ≤ k ≤ 9 –15 ≤ l ≤ 16
No. of reflections collected	7232	6574	1880
No. of independent reflections (R _{int})	3805	3953	1595
No. of data/restraints/parameters	7926/0/343	8026/0/460	3762/0/235
Goodness-of-fit on F ²	1.226	1.295	1.712
R ₁ ^a , wR ₂ ^b [(I > 2σ(I))]	0.0681, 0.1099	0.0661, 0.1567	0.0411, 0.1194
R ₁ ^a , wR ₂ ^b (all data)	0.1320, 0.1052	0.1383, 0.1765	0.0691, 0.1412
Largest difference in peak/hole (e Å ⁻³)	0.280, –0.283	0.345, –0.283	0.408, –0.376

^a R₁ = Σ||F_o| – |F_c||/Σ|F_o|.^b R₂ = [Σw(|F_o² – |F_c²||)/Σw|F_o²|]^{1/2}.**Table 2**
Bond length (Å) and angles (°) for **1**.

Bond length (Å)	(Exp.)		(Cal.)		
S(1)–C(8)	1.719(7)	1.771	C(8)–S(1)–C(9)	86.8(3)	85.7
S(1)–C(9)	1.736(7)	1.772	S(1)–C(8)–N(1)	114.9(6)	114.2
N(1)–N(2)	1.393(9)	1.368	S(1)–C(9)–N(2)	113.6(6)	113.7
N(1)–C(8)	1.293(8)	1.291	C(9)–N(2)–N(1)	112.9(6)	112.7
N(2)–C(9)	1.292(9)	1.302	C(9)–N(3)–C(10)	126.7(6)	129.5
N(3)–C(9)	1.294(9)	1.366	C(11)–C(10)–N(3)	121.4(3)	123.6
C(10)–N(3)	1.404(9)	1.409	C(7)–C(8)–S(1)	119.5(5)	123.9

filtered off and washed with water and ether ((50:50 v/v). The mixture of 4-phenyl-1-(2-phenylacetyl) thiosemicarbazide (0.285 g, 1 mmol) and Mn(NO₃)₂·4H₂O (0.251 g, 1 mmol) was heated for 4 h at 45 °C. After cooling, the reaction mixture was filtered off

Table 3
Hydrogen bond parameters [Å and °] for **1**.

D–H···A	d(D–H)	d(H···A)	d(D···A)	<(DHA)
<i>Intermolecular hydrogen bonding</i>				
C22–H22A···N1	0.970	2.398	2.994	119.18
C22–H22B···N1	0.970	2.694	2.994	93.38
C22–H22A···N6	0.970	2.684	3.649	173.33
N6–H6···N2	0.860	2.117	2.959	165.91
N3–H3A···N5	0.860	2.115	2.958	166.73
C7–H7A···N4	0.971	2.416	3.002	118.48
C7–H7B···N4	0.969	2.691	3.002	99.21
C7–H7B···N3	0.969	2.711	3.676	173.00
<i>Intramolecular hydrogen bonding</i>				
C5–H5···N1	0.930	2.575	3.070	113.67
C11–H11···N2	0.930	2.667	3.112	110.94
C20–H20···N4	0.930	2.589	3.091	114.36
C26–H26···N5	0.930	2.652	3.112	111.23

Table 4
Bond length (Å) and angles (°) for **2**.

Bond length (Å)	(Exp.)		(Cal.)		
S1–C8	1.700(5)	1.748	C8–N1–N2	111.5(5)	113.41
S1–C7	1.699(6)	1.756	C7–N2–N1	110.8(5)	113.52
N1–C8	1.188(7)	1.303	N1–C8–C9	122.9(4)	124.37
N1–N2	1.372(6)	1.354	N1–C8–S1	119.5(5)	113.75
N2–C7	1.317(6)	1.309	C9–C8–S1	117.4(4)	121.86
C9–N3	1.308(7)	1.341	N2–C7–C6	123.2(5)	122.94
N3–C13	1.333(8)	1.332	C3–C4–C5	123.9(7)	120.15

and kept for crystallization whereupon yellow crystals of **1** suitable for X-ray analyses were obtained after 15 days. Yield: 85%. m.p. 220 °C. Anal. Found. C, 67.34%; H, 4.88%; N, 15.69%; S, 11.96%. Calc. for C₁₅H₁₃N₃S (267.35): C, 67.33%; H, 4.86%; N, 15.71%; S, 11.97%. IR (KBr, cm⁻¹): ν(NH) 3270; ν(C=N) 1590; ν(N–N) 1097; ν(C–S) 794. ¹H NMR (DMSO-d₆; δ ppm): 11.48 (s, 1H, NH), 3.34 (2H, –CH₂), 7.90–6.86 (m, aromatic protons). ¹³C NMR (DMSO-d₆; δ ppm): 179.65 (C–S), 168.35 (C=O), 121.68–144.32 (aromatic carbons), 36.95 (CH₂).

2.2.2. Synthesis of 2-(5-phenyl-1,3,4-thiadiazol-2-yl)pyridine (Pthp, **2**)

The N'-benzothioylpicolinohydrazide was prepared by dropwise addition of benzodithioyl acetic acid into a methanol suspension of picolinic acid hydrazide (2.742 g, 20 mmol) in the presence of 1N NaOH with continuous stirring for 1 h. The white solid obtained was filtered, washed with water, dried and recrystallized from MeOH–CHCl₃ mixture (50:50 v/v). N'-benzothioylpicolinohydrazide (0.257 g, 1 mmol) was dissolved in water ethanol mixture (50:50, v/v) and an aqueous solution of Mn(NO₃)₂·4H₂O (0.251 g, 1 mmol) was added to the above solution and stirred for 1 h. Yellow clear solution was filtered off and kept for crystallization. Light yellow crystals of **2** suitable for X-ray

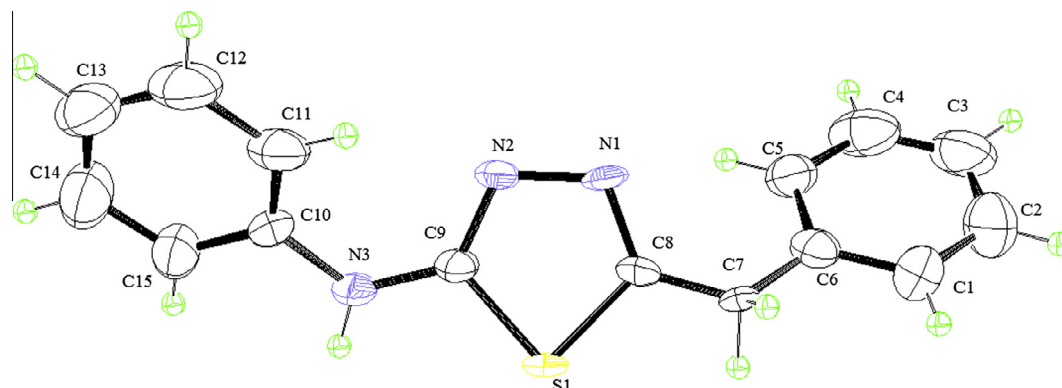


Fig. 1. ORTEP diagram of 5-benzyl-N-phenyl-1,3,4-thiadiazol-2-amine (**1**) showing atomic numbering scheme with ellipsoid of 30% probability.

Table 5
Hydrogen bond parameters (Å and °) for **2**.

D—H···A	d(D—H)	d(H···A)	d(D···A)	<(DHA)
<i>Intermolecular hydrogen bonding</i>				
C23—H23···N1	0.930	2.718	3.548	149.12
C27—H27···N8	0.927	2.605	3.387	142.13
<i>Intramolecular hydrogen bonding</i>				
C10—H10···N1	0.930	2.663	2.917	96.35
C1—H1···N2	0.931	2.642	2.920	97.97
C5—H5···S1	0.930	2.692	3.094	106.92

Table 6
Bond length (Å) and angles (°) for **3**.

Bond length (Å)	Bond length (Å)		Bond angles (°)		
	(Exp.)	(Cal.)	(Exp.)	(Cal.)	
S2—C3	1.778(11)	1.758	C3—N2—N1	110.2(12)	113.2
N2—N1	1.383(2)	1.369	S1—C3—S2	119.0(6)	119.4
S2—C4	1.749(14)	1.775	N2—C3—S2	124.4(10)	126.6
N1—C2	1.291(2)	1.293	N2—C3—S1	116.4(9)	113.9
N3—N4	1.369(17)	1.367	C5—S3—C4	84.8(7)	85.4
N3—C4	1.272(2)	1.297	N4—C5—S3	116.1(9)	114.1
S1—C2	1.751(17)	1.767	S3—C4—S2	129.1(10)	130.0
N2—C3	1.287(17)	1.296	N3—C4—S2	116.7(11)	115.1
S1—C3	1.686(13)	1.756	N3—C4—S3	114.2(10)	113.7
S3—C4	1.744(15)	1.753	C1—C2—S1	128.0(12)	125.7
S3—C5	1.713(14)	1.758	C4—N3—N4	112.2(12)	112.9
C5—N4	1.301(2)	1.299	N4—C5—C6	125.1(11)	123.2

analyses were obtained by slow evaporation of the above solution over a period of 15 days. Yield: 78%; m.p. 180 °C. Anal. Found: C, 65.21%; H, 3.71%; N, 17.56%; S, 13.40%. Calc. for C₁₃H₉N₃S (239.30) C, 65.19%; H, 3.76%; N, 17.55%; S, 13.39%. IR (KBr, cm⁻¹): ν(C=N) 1576; ν(N—N) 1073; ν(C—S) 764. ¹H NMR (DMSO-d₆; δ ppm): 7.20–8.68 (m, aromatic protons). ¹³C NMR (DMSO-d₆; δ ppm): 197.55 (C—S), 165.40 (C=N), 125.26–143.18 (aromatic carbons).

2.2.3. Synthesis of 2-(5-methyl-1,3,4-thiadiazole-2-ylthio)-5-methyl-1,3,4-thiadiazole (Mtmth, **3**)

Mn(OAc)₂·4H₂O (0.125 g, 0.5 mmol) was added to a methanol–acetonitrile suspension of 5-methyl-1,3,4-thiadiazole-2-thiol (0.101 g, 1 mmol) and the reaction mixture refluxed for 2 h. The clear solution obtained upon cooling was filtered off and kept for crystallization. Colorless crystals of **3** suitable for X-ray analyses were obtained by slow evaporation of the above solution over a period of 10 days. Yield: 70%. m.p. 192 °C. Anal. Found: C, 31.24%; H, 2.60%; N, 24.33%; S, 41.66%. Calc. for C₆H₆N₄S₃

Table 7
Hydrogen bond parameters (Å and °) for **3**.

D—H···A	d(D—H)	d(H···A)	d(D···A)	<(DHA)
<i>Intermolecular hydrogen bonding</i>				
C7—H7A···N5	0.958	2.554	3.501	169.67
C7—H7A···N6	0.958	2.456	3.395	158.51
C6—H6A···N3	0.961	2.346	3.284	165.07
C6—H6B···N4	0.961	2.546	3.476	162.76

(230.36): C, 31.25%; H, 2.61%; N, 24.31%; S, 41.68%. Found: IR (KBr, cm⁻¹): ν(C=N) 1602; ν(N—N) 1065; ν(C—S) 727. ¹H NMR (DMSO-d₆; δ ppm): 2.50 (3H, —CH₃). ¹³C NMR (DMSO-d₆; δ ppm): 190.31 (C—S), 168.80 (C=N), 38.66 (CH₃).

3. Crystal structure determination

Crystals suitable for X-ray analyses of the compounds **1**, **2** and **3** were grown at room temperature. The crystal data were collected on an Oxford Gemini diffractometer equipped with a CrysAlis CCD software using a graphite mono-chromated Mo Kα (λ = 0.71073 Å) radiation source at 293 K for **1**, **2** and **3**. Multi scan absorption correction was applied to the X-ray data collection for all the compounds. The structures were solved by direct methods (SHELXS-08) and refined against all data by full matrix least-square on F² using anisotropic displacement parameters for all non-hydrogen atoms. All hydrogen atoms were included in the refinement at geometrically ideal position and refined with a riding model [14]. The MERCURY package and ORTEP-3 for Windows program were used for generating structures [15,16].

4. Results and discussion

The compounds 5-benzyl-N-phenyl-1,3,4-thiadiazol-2-amine (**1**) and 2-(5-phenyl-1,3,4-thiadiazol-2-yl) pyridine (**2**) were obtained by the reactions of 4-phenyl-1-(2-phenylacetyl) thiosemicarbazide and N'-benzothioylpicolinohydrazide, respectively, with Mn(NO₃)₂·4H₂O whereas compound **3** was obtained by the reaction of 5-methyl-1,3,4-thiadiazole-2-thiol with Mn(OAc)₂·4H₂O via condensation of two moles of thiadiazole-2-thiol. The Schemes 1–3 depict the formation of the compounds **1**, **2** and **3**. All the compounds are air stable, non-hygroscopic crystalline solids, which are soluble in common organic solvents and can be kept at room temperature over a prolonged period without any sign of decomposition. The compounds **1**, **2** and **3** melt at 220, 180 and 192 °C, respectively. Thus, the new route employed for the syntheses of above compounds do not only impart good yields but is also adequate for growing their crystals.

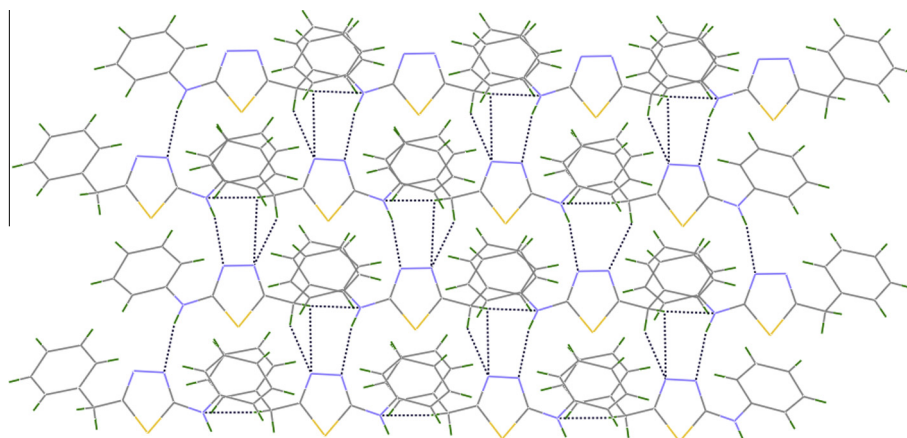


Fig. 2. Intermolecular C–H...N and N–H...N interactions forming a supramolecular architecture.

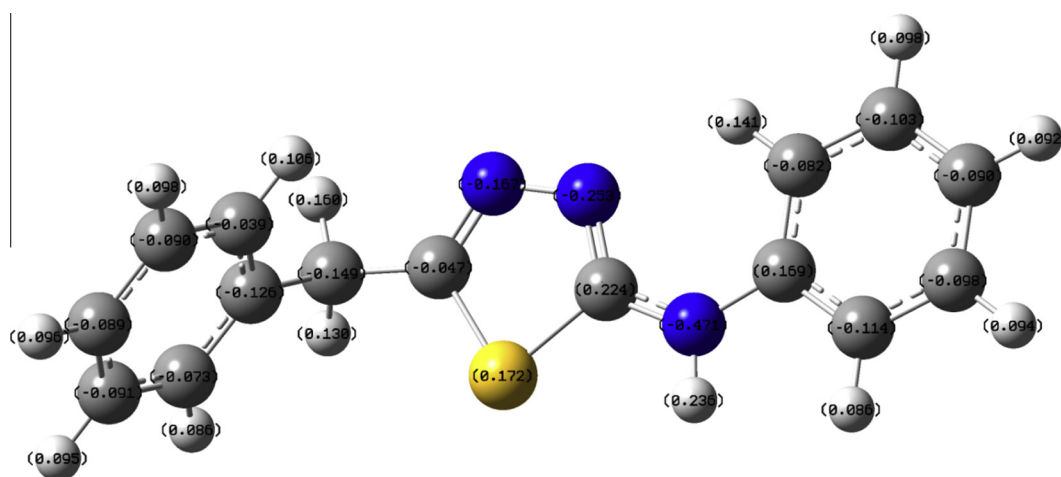


Fig. 3. Optimized geometry and charge distribution on 5-benzyl-N-phenyl-1,3,4-thiadiazol-2-amine (1).

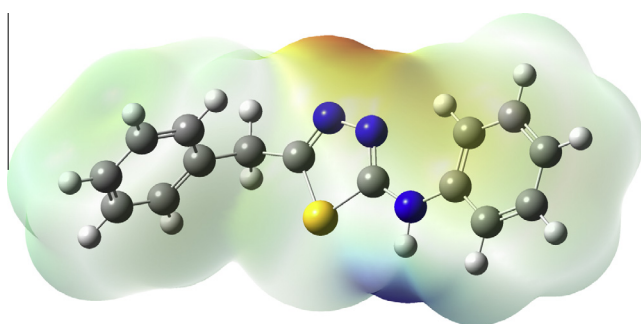


Fig. 4. MEP plot of 5-benzyl-N-phenyl-1,3,4-thiadiazol-2-amine (1).

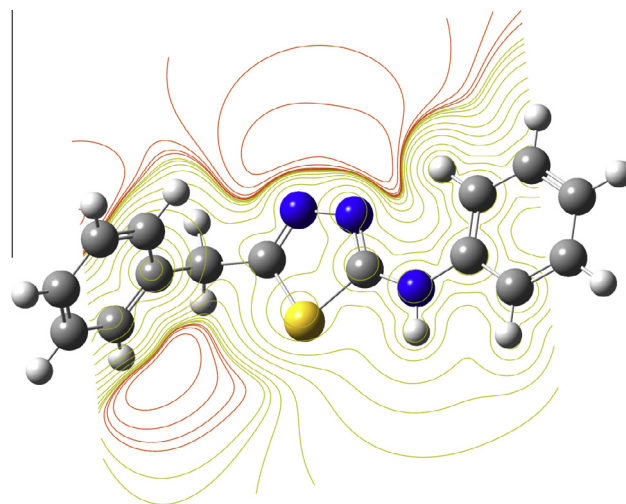


Fig. 5. Contour map of 5-benzyl-N-phenyl-1,3,4-thiadiazol-2-amine (1).

4.1. IR spectra

The IR spectra of the compounds **1** and **2** in KBr show absorptions (cm^{-1}) due to the stretching modes of NH (3270, only for **1**), C=N (1590, 1576), C–S (794, 764) and N–N (1097, 1073). The bands at 764 and 677 cm^{-1} in compound **2** are due to the pyridine and phenyl rings, respectively. The IR spectrum of the compound **3** is expected to give rise to characteristic bands due to $\nu(\text{C}=\text{N})$, $\nu(\text{N}=\text{N})$, and $\nu(\text{C}=\text{S})$ which occur at 1602, 1065 and 812 cm^{-1} , respectively [17].

4.2. ^1H and ^{13}C NMR spectra

The ^1H NMR spectrum of Bptha (**1**) exhibits two signals at δ 11.48 and 3.34 ppm for the amine and CH_2 protons, respectively and the phenyl ring protons appear as a multiplet between δ 7.90 and 6.86 ppm. The ^{13}C spectrum of Bptha (**1**) shows signals

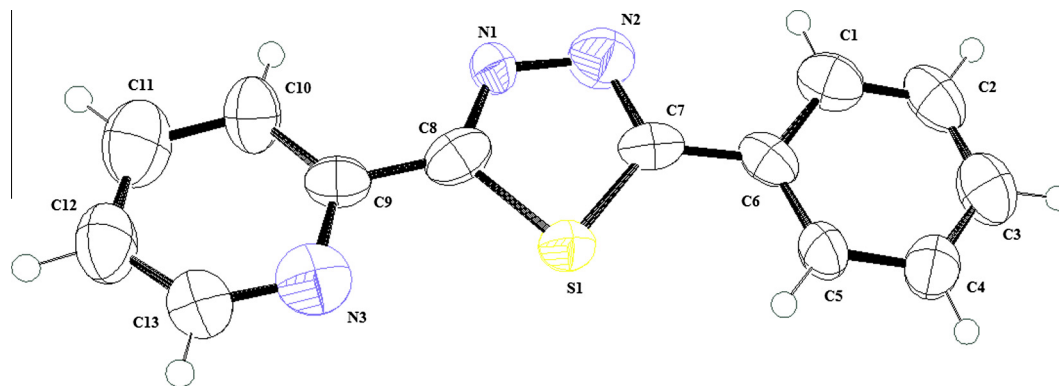


Fig. 6. ORTEP diagram of 2-(5-phenyl-1,3,4-thiadiazol-2-yl)pyridine (**2**) showing atomic numbering scheme with ellipsoid of 30% probability level.

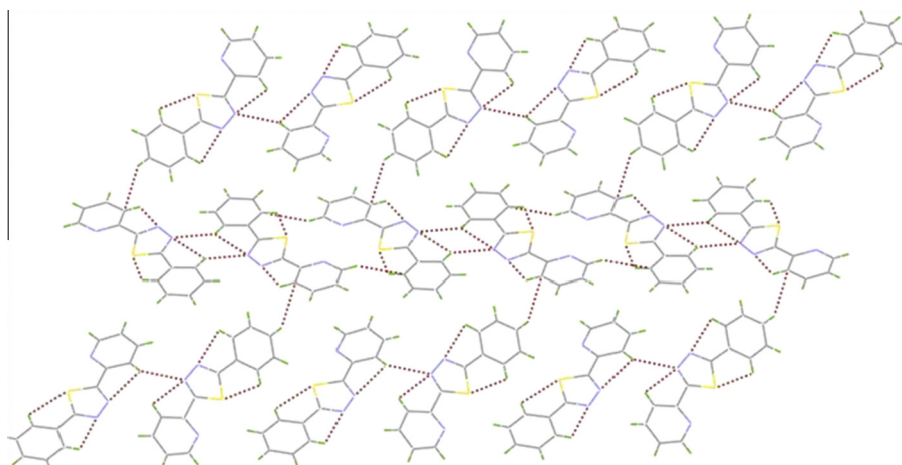


Fig. 7. Intermolecular C–H...N interactions and intramolecular C–H...N and C–H...S interactions in **2**.

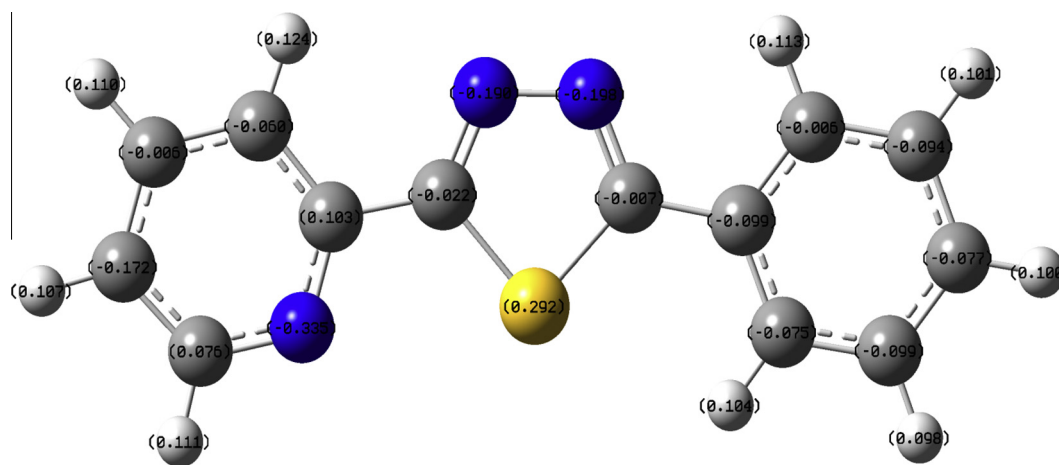


Fig. 8. Optimized and charge distribution on 2-(5-phenyl-1,3,4-thiadiazol-2-yl)pyridine.

at δ 179.65, 168.35 and 121.68–144.32 ppm due to C–S, C=N and phenyl ring carbons. The NMR data thus indicates that the compound 5-benzyl-N-phenyl-1,3,4-thiadiazol-2-amine (**1**) is present in the cyclic form. The ^1H NMR spectrum of Pthp (**2**) exhibits signals for aromatic protons between δ 7.20 and 8.68 ppm. The ^{13}C spectrum of **2** shows signals at δ 197.55 and 165.40 ppm due to C–S and C=N carbons, respectively. The phenyl and pyridine ring carbons appear in the region of 125.26–143.18 ppm. The ^1H NMR spectrum of Mtmth (**3**) in DMSO- d_6 shows signal at 2.50 ppm

due to methyl protons. The signals appearing at 190.31, 168.80 and 38.66 ppm in the ^{13}C NMR spectrum of **3** are due to the $>\text{C}=\text{S}$, $>\text{C}=\text{N}$ and CH_3 carbons, respectively.

4.3. Crystal structure descriptions of **1**, **2** and **3**

The crystallographic data and structural refinement details for compounds **1**, **2** and **3** are given in Table 1. Selected bond distances and bond angles are compiled in Tables 2, 4 and 6. Fig 1, 6 and 11

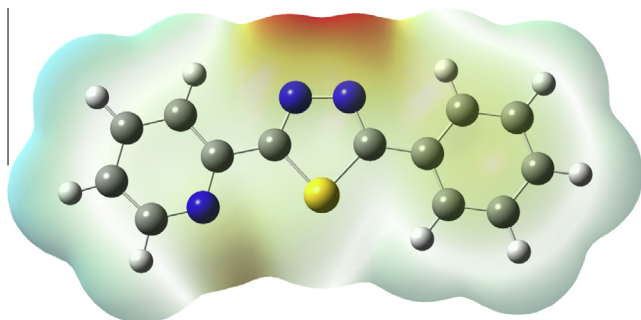


Fig. 9. MEP plot of 2-(5-phenyl-1,3,4-thiadiazol-2-yl)pyridine.

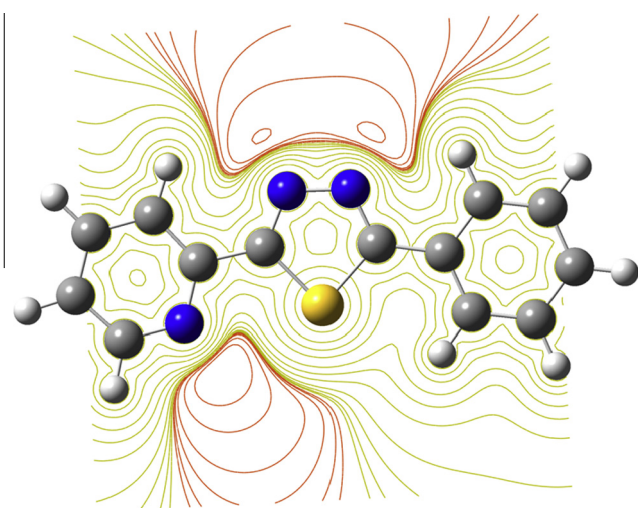


Fig. 10. Contour map of 2-(5-phenyl-1,3,4-thiadiazol-2-yl)pyridine.

show the ORTEP diagrams of the compounds **1**, **2** and **3** with their atomic numbering scheme. The C–S, N–N and C–N bond distances of compounds **1**, **2** and **3** are shorter than the corresponding single bond distance. This fact suggests multiple bond order and confers aromaticity to the ring and C–S bond in thiadiazole ring involves carbon atom with sp^2 hybridization. This result is similar to those found for 2,5-bis(2-pyridyl)-1,3,4-thiadiazole [18], 5-(4-hydroxyphenyl)-1,3,4-thiadiazole-2-thiol [19] and 4(5-ethyl sulfanyl-1,3,4-thiadiazole-2-yl)-pyridinium perchlorate [11]. Deviation of

the bond angle from 120° in the 1,3,4-thiadiazole ring is a common feature in five-membered rings. The values found for bond angles and lengths measured for **1**, **2** and **3** are similar to those reported in related compounds [18,19]. The dihedral angle between the thiadiazole and the phenyl rings is found to be 43.85° for compound **1** indicating that both rings are tilted with respect to each other whereas for compound **2**, the dihedral angle between the thiadiazole and the phenyl rings is 5.05° and thiadiazole and pyridine rings are almost coplanar to the thiadiazole ring. For compound **3**, the dihedral angle between both thiadiazole rings is 1.48° indicating that both rings are almost coplanar. Bond lengths and angles in the phenyl ring and thiadiazole ring for compounds **1** and **2** are generally normal. The geometrical parameters relevant for these interactions are given in Tables 3, 5 and 7. In the solid state, the compound **1** is stabilized via intermolecular C–H...N and N–H...N interaction between thiadiazole ring nitrogen and CH_2 and NH hydrogen atoms substituted at 2 and 5 positions of the thiadiazole ring, which leads to the formation of linear chain structure (Fig. 2). In addition, the structure of compound **2** is stabilized by C–H...N interaction occurring between thiadiazole ring nitrogen with hydrogens of phenyl ring. The compound **2** is stabilized via intermolecular C–H...N interaction between thiadiazole ring and hydrogen atoms of phenyl ring of a nearby molecule (Fig. 7). The compound **3** is stabilized via intermolecular C–H...N interaction between thiadiazole ring nitrogen and hydrogen atoms of methyl group of a nearby molecule (Fig. 12). The two neighboring molecules are also connected via S...N interaction occurring between thiadiazole ring sulfur and nitrogen in the range of 3.110–3.348 Å. The compound **2** also contains S...N as intramolecular interaction. The above observed intermolecular and intramolecular interactions have stabilized the molecular crystal packing of compounds **1**, **2** and **3**.

4.4. Geometry optimization of **1**, **2** and **3**

All calculations and the geometry optimization of 5-benzyl-N-phenyl-1,3,4-thiadiazol-2-amine (**1**), 2-(5-phenyl-1,3,4-thiadiazol-2-yl)pyridine (**2**) and 2-(5-methyl-1,3,4-thiadiazole-2-ylthio)-5-methyl-1,3,4-thiadiazole (**3**) have been performed with Gaussian 03 and Gauss View 4.1 [20] program packages using DFT method with functional B3LYP and basis set DFT/B3LYP/6-31+G(d,p) [21,22]. The input geometries of compounds for the DFT calculations were generated from single crystal X-ray data. The optimized geometrical parameters are listed in Tables 2, 4 and 6. The slight disagreement in the bond lengths and angles are due to the fact

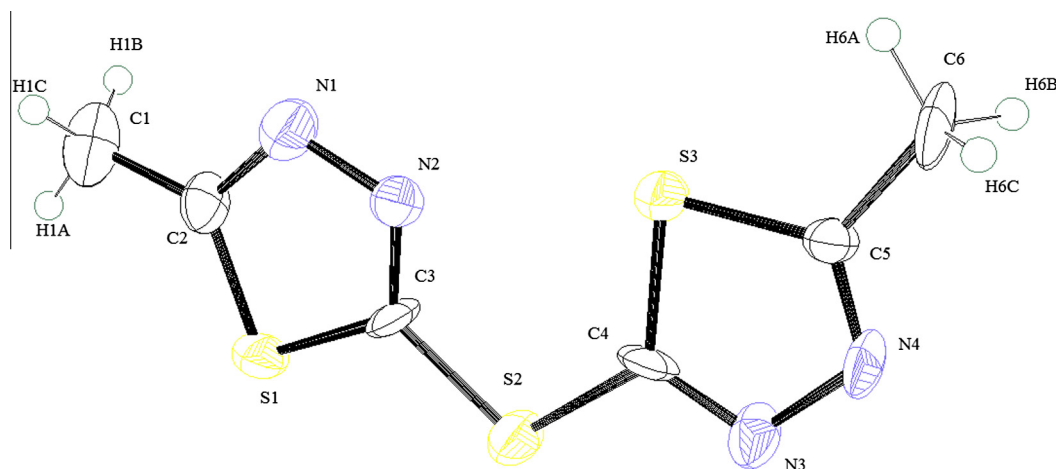


Fig. 11. ORTEP diagram of 2-(5-methyl-1,3,4-thiadiazole-2-ylthio)-5-methyl-1,3,4-thiadiazole (**3**) showing atomic numbering scheme with ellipsoid of 30% probability.

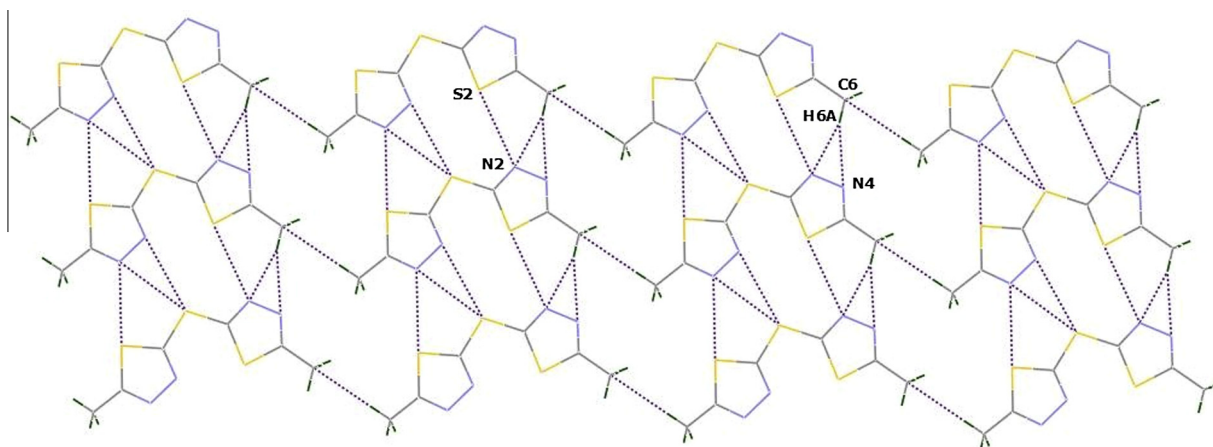


Fig. 12. Intermolecular C—H...N and S...N interactions and intramolecular S...N interactions.

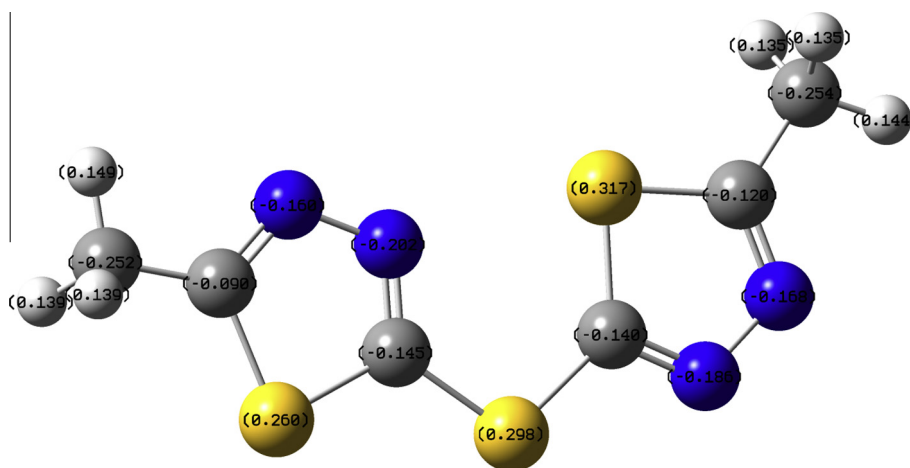


Fig. 13. Optimized and charge distribution on 2-(5-methyl-1,3,4-thiadiazole-2-ylthio)-5-methyl-1,3,4-thiadiazole (3).

that the experimental results are for the solid phase and the theoretical calculations are for the gas phase. In the solid state, the existence of a crystal field along with the intermolecular interactions connect the molecules together, which results in the differences in bond parameters between the calculated and experimental values. The optimized geometries and charge distribution on atoms of molecule are shown in Fig 3, 8 and 13.

4.5. Molecular electrostatic potential and contour maps

The molecular electrostatic potential (MEP) is a useful feature to study reactivity given that an approaching electrophile will be attracted to negative regions (the electron distribution where effect is dominant). In the majority of the MEP, while the maximum negative region with preferred site for electrophilic attack indications as red color, the maximum positive region which preferred site for nucleophilic attack symptoms as blue color. The importance of MEP lies in the fact that it simultaneously displays molecular size, shape as well as positive, negative and neutral electrostatic potential regions in terms of color grading and is very useful in research of molecular structure with its physicochemical property relationship [23]. The resulting surface simultaneously displays molecular size and shape and electrostatic potential value. MEP plot of compounds 1, 2 and 3 are shown in Fig. 4, 9 and 14 respectively. The MEP is a plot of electrostatic potential mapped onto the constant electron density surface. The different values of the electrostatic potential at the surface are represented by different colors. Potential increases in the order red < orange < yellow < green < blue. The color code of these maps is in the range between -0.05431 a.u. (deepest red) and 0.05431 a.u. (deepest blue) in compound, where blue indicates the strongest attraction and red indicates the strongest repulsion. Regions of negative $V(r)$ are usually associated with the lone pair of electronegative atoms. As can be seen from the MEP map of the molecule, while regions having the negative

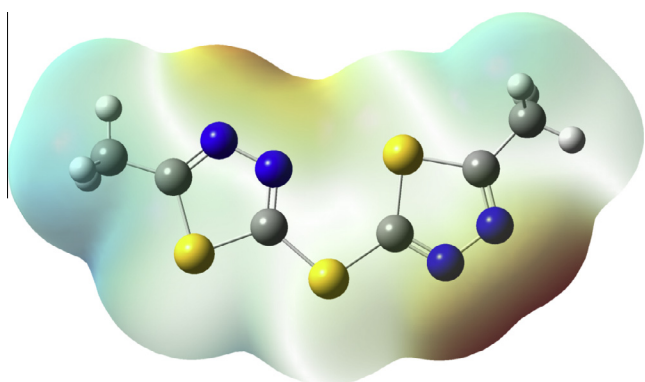


Fig. 14. MEP plot of 2-(5-methyl-1,3,4-thiadiazole-2-ylthio)-5-methyl-1,3,4-thiadiazole (3).

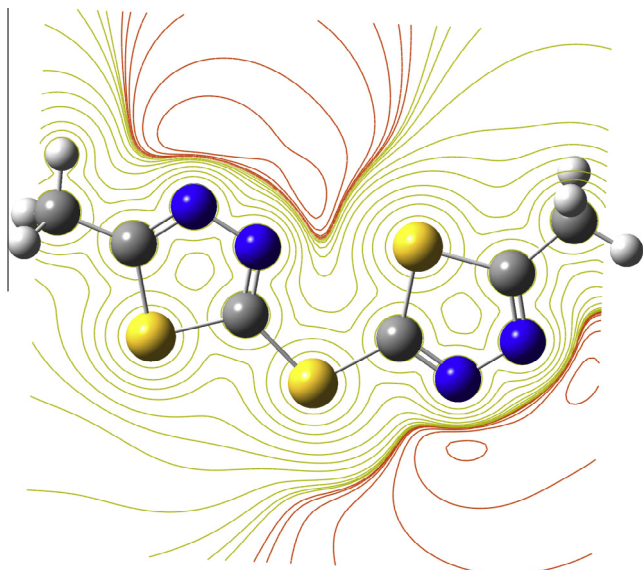


Fig. 15. Contour map of 2-(5-methyl-1,3,4-thiadiazole-2-ylthio)-5-methyl-1,3,4-thiadiazole (**3**).

Table 8
Calculated Frontier Molecular Orbitals energies (eV) for the compounds **1**, **2** and **3**.

Compound	Energies (Hartree)			ΔE (Hartree)	Degree of hardness η
	HOMO	LUMO	(eV)		
1	-0.03693	-0.21556	4.86077	2.43039	
2	-0.08250	-0.23770	3.67898	1.83949	
3	-0.06061	-0.24451	5.00417	2.50209	

potential are over the electronegative atom (nitrogen atom), the regions having the positive potential are over the hydrogen atoms. A maximum positive region localized on the H atoms in the ring.

However, the H atoms at the CH₃ group have smaller values than on the H atoms in the ring. From this result, we can say that the H atoms indicate the strongest attraction and N atoms indicate the strongest repulsion.

A contour map is a two-dimensional XY plot of a three-dimensional XYZ surface showing lines where the surface intersects planes of constant elevation (Z). The contour maps are also used to show lines of constant density or brightness, such as electrostatic potentials. The contour maps are also calculated by DFT/B3LYP/6-31+G(d,p) method at the 0.02 isovalues and 0.004 density values at the same level of calculations of the MEP mapped surface of the molecules. The contour maps of the molecules are shown in Fig 5, 10 and 15. The contour maps of the compounds show that there is more electron density around the thiadiazole ring nitrogen.

4.6. Frontier molecular orbital analysis

Frontier molecular orbitals (FMOs) refer to the highest occupied molecular orbital (HOMO) and the lowest unoccupied molecular orbital (LUMO) which are very popular quantum chemical parameters that determine the molecular reactivity and offer qualitative prediction of the excitation properties and the ability of electron transport [24,25]. The outermost higher energy orbital (HOMO) acts as an electron donor while the lowest energy orbital (LUMO) acts as an electron acceptor. The energies of these orbitals of the molecule calculated by using DFT/B3LYP method are found to be negative (Table 8), which indicate that the molecules are stable [26]. The isodensity surface plots of HOMO and LUMO for the compounds are shown in Fig. 16. The positive phases are red and the negative ones are green. It can be seen from Fig. 16 that the electron density of HOMO in case of compound **1** is localized on the thiadiazole and N-phenyl rings, while the LUMO is localized on the entire three rings (Fig. 16). The electron density of HOMO in case of compound **3** is localized on the thiadiazole ring and methyl group, while the LUMO is not localized on the methyl group. On the other hand, the HOMO–LUMO electron density for the compound **2** is located over the aryl group and thiadiazole ring. Compound **2**

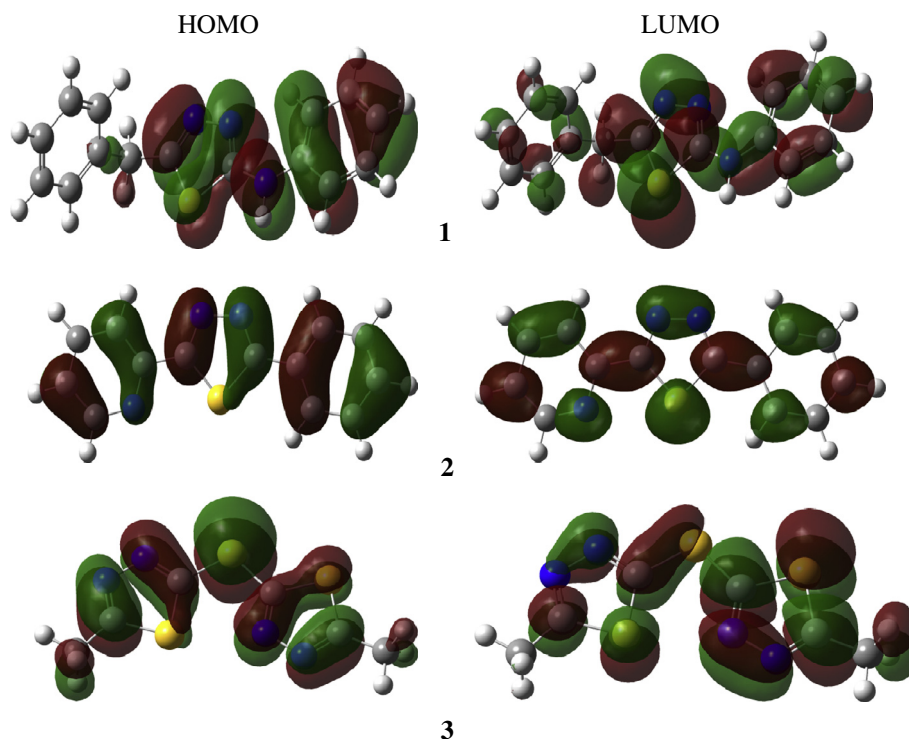


Fig. 16. Ground state isodensity surface plots for molecular orbitals of the compounds **1**, **2** and **3**.

makes larger contribution to HOMO and LUMO than those of compounds **1** and **3**, due to the presence of thiadiazole ring acting as a π -conjugation bridge. The above results indicate that compound **2** has better chemical activity and may effectively carry out intramolecular charge transfer upon excitation. The electronic transition from the ground state to the excited state takes place due to a transfer of electrons from the HOMO to LUMO levels and is mainly associated with the $\pi \rightarrow \pi^*$ transition. The chemical hardness and softness of a molecule is a good indication of the chemical stability of a molecule. From the HOMO-LUMO energy gap, one can find whether the molecule is hard or soft. The molecules having a large energy gap are known as hard and molecules having a small energy gap are known as soft molecules. The soft molecules are more polarizable than the hard ones, because they need small energy for excitation. The hardness value of a molecule can be determined by the formula [27]

$$\eta = \{-\varepsilon_{\text{HOMO}} + \varepsilon_{\text{LUMO}}\}/2$$

where $\varepsilon_{\text{HOMO}}$ and $\varepsilon_{\text{LUMO}}$ are the energies of the HOMO and LUMO molecular orbitals. The value of η for the title compounds **1**, **2** and **3** are 2.43039, 1.83949 and 2.50209 eV, respectively. From the above values, it can be concluded that the compounds **1**, **2** and **3** are hard materials and out of these, the compound **2** is a less hard material than compounds **1** and **3**.

4.7. Non-linear optical (NLO) properties

The non-linear optical (NLO) properties of materials associated with the delocalized π -electrons of a molecule play an important role in the design of materials used in communication technology and optical devices [28]. An increase in conjugation on the molecule is resulted in the change in the NLO properties which in turn are related to the energy gap between HOMO and LUMO. An addition of substituent to the conjugated systems of organic molecules could affect the nonlinear optical properties by changing the energy gap between HOMO and LUMO where the small HOMO-LUMO gap requires small excitation energy and so the absorption bands of a molecule are shifted towards the visible region [29,30]. It is found that, in compound **2**, the presence of phenyl and pyridyl ring on the thiadiazole ring at 2 and 5 positions, decreases the value of the energy gap, so the absorption bands in the electronic spectrum of **2** is shifted towards the visible region and consequently, increases the nonlinear optical properties as compared to compounds **1** and **3**. The structural differences between compounds **1**, **2** and **3** are only in the substituted groups at positions 2 and 5 with the same thiadiazole ring and this difference has little effects on the constituents of the Frontier Molecular Orbital. The energy gap of compounds **1**, **2** and **3** are 4.86077, 3.67898 and 5.00417 eV, respectively.

5. Conclusion

This paper reports the syntheses, spectral, structural investigations and DFT calculations of 5-benzyl-N-phenyl-1,3,4-thiadiazol-2-amine (**1**), 2-(5-phenyl-1,3,4-thiadiazol-2-yl)pyridine (**2**) and 2-(5-methyl-1,3,4-thiadiazole-2-ylthio)-5-methyl-1,3,4-thiadiazole (**3**). During the course of the reaction, substituted thiosemicarbazide/thiohydrazide got cyclized into the corresponding thiadiazole in the presence of a manganese(II) nitrate via loss of H₂O for compounds **1** and **2**. This strategy has been found to be an easy and facile route to synthesize new thiadiazole compounds from substituted thiosemicarbazide/thiohydrazide. However, condensation occurred in the case of a already cyclized compound 5-methyl-1,3,4-thiadiazole-2-thiol which yielded 2-(5-methyl-1,3,4-thiadiazole-2-ylthio)-5-methyl-1,3,4-thiadiazole (**3**) by loss of one mole of H₂S from two moles of 5-methyl-1,3,4-thiadia-

zole-2-thiol. The compounds are stabilized through intramolecular and weak intermolecular hydrogen bonding. X-ray crystallographic results are well produced by DFT calculations. MEP mapped surfaces and the contour maps of molecule are computed by same method. The MEP and the contour map show the negative potential (red region) sites on nitrogen atoms and positive potential (blue region) sites around the hydrogen atoms. The HOMO and LUMO energies of the molecules are negative indicating that the all compounds are stable. The lower energy gap for the compound **2** indicates better NLO properties as compared to compounds **1** and **3**.

Acknowledgements

Dr. S.K. Kushawaha is thankful to the Department of Science and Technology, New Delhi, India for the award of a Young Scientist Project (No. SR/FT/CS-110/2011). R.K. Dani thanks UGC, New Delhi for the award of RGNF (SRF).

Appendix A. Supplementary material

CCDC 943021, 948324 and 943022 contain the supplementary crystallographic data for compounds **1**, **2** and **3**. These data can be obtained free of charge from the Cambridge Crystallographic Data Center via www.ccdc.cam.ac.uk/data_request/cif. Supplementary data associated with this article can be found, in the online version, at <http://dx.doi.org/10.1016/j.molstruc.2013.09.051>.

References

- [1] S.K. Sonwane, S.D. Srivastava, Proc. Natl. Acad. Sci. India 78A (II) (2008) 29–136.
- [2] R.S. Laxmi, N.S. Shetty, R.R. Kamble, I.A.M. Khazi, Eur. J. Med. Chem. 44 (2008) 2828–2833.
- [3] A. Foroumadi, S. Emami, A. Hassanzadeh, M. Rajaei, K. Sokhanvar, M.H. Moshafi, A. Shafiee, Bioorg. Med. Chem. Lett. 15 (2005) 4488–4492.
- [4] B.L. Sharma, S.K. Tandon, Pharmazie 39 (1984) 858–859.
- [5] T. Onkol, D.S. Doruer, L. Uzun, S. Adek, S. Ozkan, M.F. Ahin, J. Enzyme Inhib. Med. Chem. 23 (2008) 277–284.
- [6] V. Mathew, J. Keshavayya, V.P. Vaidya, D. Giles, Eur. J. Med. Chem. 42 (2007) 823–840.
- [7] Q. Bano, N.T. Nizamudin, Indian J. Chem. 31B (1992) 714–718.
- [8] S.H. Joshi, M.K. Thaker, J. Vet. Sci. 4 (2011) 152–164.
- [9] N. Siddiqui, A. Rana, S.A. Khan, M.A. Bhat, S.E. Haque, Med. Chem. Lett. 17 (2007) 4178–4182.
- [10] E. Jedlovska, J. Lesko, Synth. Commun. 24 (1994) 1879–1885.
- [11] J.P. Jasinski, M.K. Bharty, N.K. Singh, S.K. Kushawaha, R.J. Butcher, J. Chem. Crystallogr. 41 (2011) 6–11.
- [12] S. Jalhan, A. Jindal, A. Gupta, Hemraj, Asian J. Pharm. Clin. Res. 5 (2012) 199–208.
- [13] M. Barboiu, M. Cimpoesu, C. Guran, C. Supuran, Metal-Based Drug 3 (1996) 227–232.
- [14] G.M. Sheldrick, Acta Cryst. A64 (2008) 112–122.
- [15] I.J. Bruno, J.C. Cole, P.R. Edgington, M. Kessler, C.F. Macrae, P. McCabe, J. Pearson, R. Taylor, Acta Cryst. Sect. B58 (2002) 389–397.
- [16] L.J. Farrugia, J. Appl. Cryst. 45 (2012) 849–854.
- [17] G.S. Patricia, G.T. Javier, A.M. Miguel, J.A. Francisco, R. Teofilo, Inorg. Chem. 41 (2002) 1345–1347.
- [18] F. Bentiss, M. Lagrenee, H. Vezin, J.P. Wignacourt, E.M. Holt, Polyhedron 23 (2004) 1903.
- [19] M.K. Bharty, A. Bharti, R.K. Dani, S.K. Kushawaha, R. Dulare, N.K. Singh, Polyhedron 26 (2012) 2597.
- [20] M.J. Frisch, G.W. Trucks, H.B. Schlegel, G.E. Scuseria, M.A. Robb, J.R. Cheeseman, V.G. Zakrzewski, J.A. Montgomery, Jr., R.E. Stratmann, J.C. Burant, S. Dapprich, J.M. Millam, A.D. Daniels, K.N. Kudin, M.C. Strain, O. Farkas, J.B.V. Tomasi, M. Cossi, R. Cammi, B. Mennucci, C. Pomelli, C. Adamo, S. Clifford, J. Ochterski, G.A. Petersson, P.Y. Ayala, Q. Cui, D.K. Morokuma, A.D. Malick, K. Rabuck, J.B. Raghavachari, J. Foresman, J. Cioslowski, J.V. Ortiz, A.G. Baboul, B.B. Stefanov, G.L.A. Liu, P. Piskorz, I. Komaromi, R. Gomperts, R.L. Martin, D.J. Fox, T. Keith, M.A. Al-Laham, C.Y. Peng, A. Nanayakkara, M. Challacombe, P.M.W. Gill, B. Johnson, W. Chen, M.W. Wong, J.L. Andres, C. Gonzalez, M. Head-Gordon, E.S. Replogle, J.A. Pople, Gaussian 03, Revision A.1, Gaussian Inc., Pittsburgh, 2003.
- [21] A.D. Becke, J. Chem. Phys. 98 (1993) 5648–5652.
- [22] C. Lee, W. Yang, R.G. Parr, Phys. Rev. B. 37 (1988) 785–789.
- [23] J.S. Murray, K. Sen, Molecular Electrostatic Potentials, Concepts and Applications, Elsevier, Amsterdam, 1996.
- [24] M. Belletete, J.F. Morin, M. Leclerc, C. Durocher, J. Phys. Chem. A 109 (2005) 6953.

- [25] D. Zhenminga, S. Hepinga, L. Yufanga, L. Dianshenga, L. Bob, *Spectrochim. Acta, Part A* 78 (2011) 1143–1148.
- [26] S.W. Xia, X. Xu, Y.L. Sun, Y.L. Fan, Y.H. Fan, C.F. Bi, D.M. Zhang, L.R. Yang, *Chin. J. Struct. Chem.* 25 (2006) 849–883.
- [27] K. Fukui, *Science* 218 (1982) 747–754.
- [28] D. Sajan, J. Hubert, V.S. Jayakumar, J. Zaleski, *J. Mol. Struct.* 785 (2006) 43–53.
- [29] K.S. Thanthiriwatte, K.M. Nalin de Silva, *J. Mol. Struct.* 617 (2002) 169.
- [30] R.G. Pearson, *Proc. Natl. Acad. Sci.* 83 (1986) 8440–8441.